Transactions, SMiRT-23
Manchester, United Kingdom - August 10-14, 2015
Division II, Paper ID 378

INVESTIGATIONS ON FATIGUE CRACK PROPAGATION UNDER CYCLIC ISOTHERMAL AND THERMO-MECHANICAL LOADINGS FOR A TYPE 304L STAINLESS STEEL

Patrick Le Delliou[1], Frédérique Rossillon[2], Cédric Gourdin[3], Antoine Fissolo[3], and Grégory Perez[3]

[1] EDF Research & Development Division, Moret sur Loing, France
[2] EDF, SEPTEN, Villeurbanne, France
[3] CEA DEN/DANS/DM2S/SEMT, Saclay, France

ABSTRACT

This paper deals with crack propagation under cyclic thermo-mechanical loads, as encountered in PWR piping. To compute the crack propagation rate, the French RSE-M Code requires applying a plastic correction (Irwin's correction and α coefficient) to the stress intensity factor, since austenitic steels are very ductile. Additional investigations have been conducted at CEA to improve this correction.
In a first step, an isothermal test campaign was performed on CT-specimens with various loading conditions ($0.10 \leq R \leq 0.80$), showing that the application of a plastic correction on K is not necessary.
In a second step, a new device called "PROFATH" was built. The specimen is a thick-walled 304L stainless steel tube, and cyclic loads are applied: in a first part of the cycle, the external wall is heated by a high frequency induction coil, and in a second part of the cycle, heating is stopped and the internal wall is cooled by running water. To be sure that only one crack will grow, a sharp circumferential groove is machined at the outer surface in the heated portion of the tube. A constant tensile loading is applied to the specimen. The paper describes the test set up and the instrumentation used to follow the crack propagation along the test, presents the main experimental results and finally gives their interpretation.

INTRODUCTION

In operation, components such as train wheels, engine pistons, moulds, brazing of electrical devices, or turbine blades are submitted to cyclic loads which have thermal origins (Fissolo, 2001). In nuclear power plants, thermal fatigue has firstly been observed in fast breeder reactors (FBR) and then, in some components of pressurized water reactors (PWR) (Fissolo, 2001; Nulife, 2008; Cipière, 2001). In particular, cyclic thermal loads may lead to multi-cracking, such as the thermal fatigue crazing (Fissolo, 1998). In that frame, investigations on thermal loading have been undertaken using specific devices (Ancelet, 2007; Fissolo, 1996; Fissolo, 2009; Bouin, 2010).

This present study focuses on the crack-propagation under cyclical thermo-mechanical loads, as may be encountered in Pressurized Water Reactor pipes: thermal loads may correspond to an incomplete mixing between cold and warm fluids, hot or cold thermal shocks, or thermal stratification... Mechanical loads may result from water pressure itself, or may be produced by the boundary conditions and configuration of component (i.e. bending or axial loads). In order to estimate a possible crack propagation, the French RSE-M Code proposes in Appendix 5.3 to apply a plastic correction for ductile materials (RSE-M, 2010); so, this correction concerns particularly the austenitic stainless steels (as AISI 304L steel) (RCC-MRx, 2012). In that frame, the stress intensity factor range (ΔK) is deduced from a linear elastic fracture mechanics analysis (LEFM) and then is corrected as follows:

$\Delta K_{CP} = \alpha \Delta K \sqrt{\frac{a + r_y}{a}}$ where: $r_y = \frac{1}{6\pi}\left(\frac{\Delta K}{2S_y}\right)^2$, and S_y is the 0.2 % yield stress $Y_{S0.2}$.

In the case of pure thermal fatigue, α is simply taken equal to 1, whereas a α correction is requested when the mechanical part of loading becomes significant ($K_{max}^{meca} > 0.2K_{max}$):

- $\alpha = 1$ when $r_y \le 0.05\,(W-a)$
- $\alpha = 1 + 0.15\left[\dfrac{r_y - 0.05\,(W-a)}{0.035\,(W-a)}\right]$ when $0.05\,(W-a) < r_y \le 0.085\,(W-a)$
- $\alpha = 1{,}15$ when $r_y > 0.085(W-a)$

However, such methodology must be improved, particularly in the cases of cyclic thermo-mechanical loads. For nuclear components, thermal loading corresponds to restraint to thermal expansion, and thus mainly to strain-controlled loading. In that frame, crack propagation leads to some mechanical unloading in the un-cracked zone. In such way, methodologies based only on load-controlled tests cannot be very efficient.

In order to improve the estimation of crack propagation under cyclic thermal loading, a new device called PROFATH has been built in CEA laboratory. In that one, specimens are submitted in the same time to cyclic thermal load and to constant tensile load. This paper details the preparation of the tests and the first thermal maps obtained on this new device. However, present study begins with a crack propagation campaign performed for isothermal conditions on CT specimens.

CRACK PROPAGATION TESTS CONDUCTED UNDER ISOTHERMAL CONDITIONS

Seven CT specimens (five CT25 and two CT50) were tested with different load ratios ($0.10 \le R \le 0.80$). The condition of validity given by ASTM E 647 (ASTM, 1995) and AFNOR A 03-404 (AFNOR, 1991) test standards is:

$$W - a \ge \frac{4}{\pi}\left(\frac{K_{MAX}}{S_y}\right)^2$$

where $W - a$ is the uncracked length: ahead of the crack, the plastic zone evaluated from the monotonous part of loading (Irwin's relation) must be eight times smaller than the uncracked length.

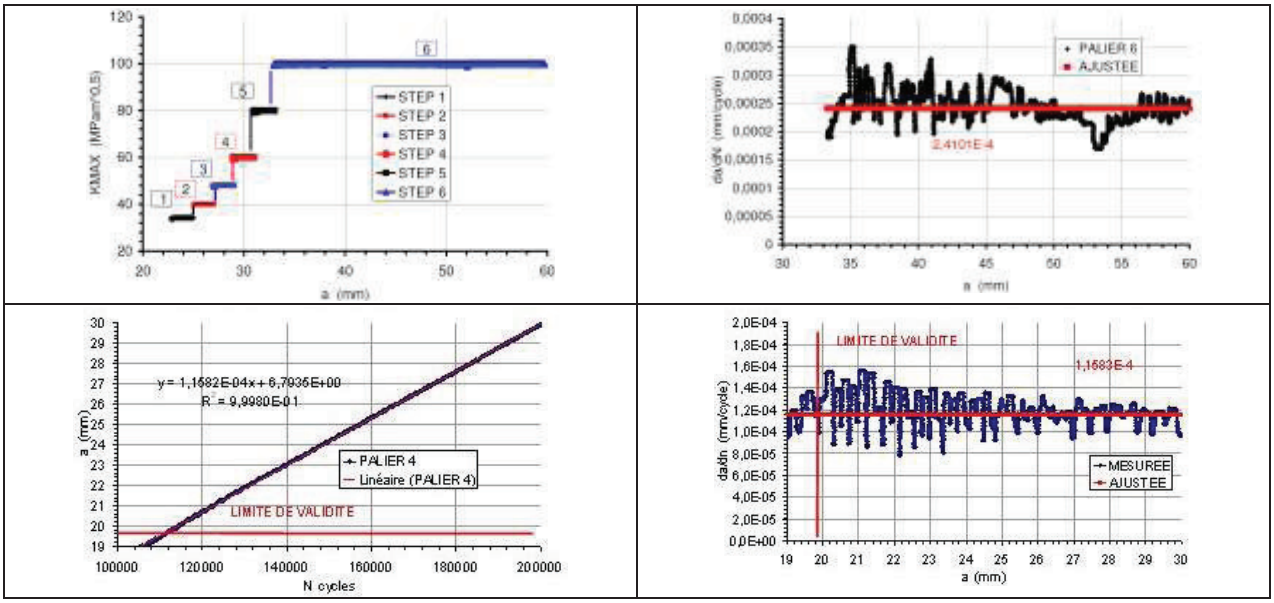

Figure 1. Tests performed at room temperature on 304L austenitic stainless steel CT specimens, with several loading steps (for each step, the crack is propagated with constant ΔK and K_{max} values).

Fig. 1 gives example of two test results. The two upper graphs correspond to a CT50 test performed with 6 steps and a load ratio R=0.6 for the last step. The two lower graphs correspond to a CT25 test performed with 4 steps and a ratio R of 0.7 for the last step. Fig. 1 shows that present condition of validity appears to be excessive in our case: the condition of validity is not verified for the last two steps for the first test (5th and 6th step from 30 mm), and for the last step for the second test (4th step from 20 mm). All the results confirm plainly such evolution, since ΔK_{eff} results remain coherent even when the uncracked length is two times smaller than the required condition (Fig. 2). Furthermore, both the plastic parameter α and the crack-length (r_y) corrections proposed by the RSE-M code are not necessary, even for the maximal conditions encountered in this campaign: $r_y \approx 0.1(W-a)$. However, improvement of the code methodology requires other tests with other geometry and other type of loading.

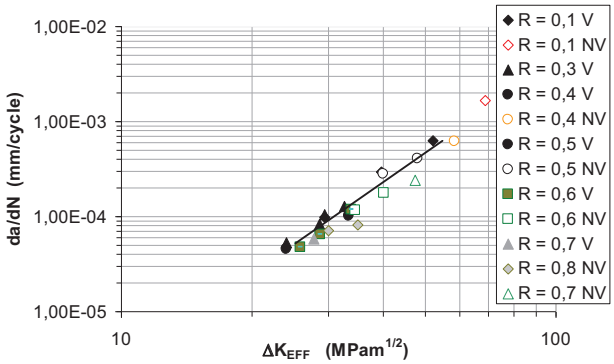

Figure 2. Results of fatigue tests performed on 304L austenitic stainless steel CT specimens at room temperature and for different values of the load ratio R ($0.10 \leq R \leq 0.80$), V=valid, NV=non valid.

PRESENTATION OF THE THERMO-MECHANICAL DEVICE PROFATH

Specimen geometry

The specimen is a thick stainless steel pipe (Fig. 3). Despite cracks appear preferentially at the inner surface for real components (such as thermal fatigue crazing), crack is placed on the external surface for practical reasons. Such configuration allows better crack opening measurements and facilitates the crack observations during the intermediate test stops. Calculation of mechanical fields with such geometry is relatively simple, since it corresponds to axis-symmetrical conditions. All the thermal and mechanical calculations have been made using finite element method; the FE software used is the CEA code Cast3M (Cast3M). Dimensions of specimen are taken as 60 mm diameter, 10 mm thickness and 300 mm length.

Thermal loading

All the preliminary test calculations were made with a 30°C-300°C thermal cycle. In order to reduce the heating phase time, an external high-frequency eddy-current heating system is placed around the crack plane. The maximum temperature of the outer surface is reached in about 30 s (Fig. 3). Then, the temperature of the external surface is maintained until the temperature radial gradient goes down close to 10°C. After, heating is stopped and water-cooling of the inner surface is started. This second phase leads to a reduction of the temperature of the outer surface to 30°C. After a very brief air injection (0.5 s) to empty the inside volume of the specimen, a new cycle can be started.

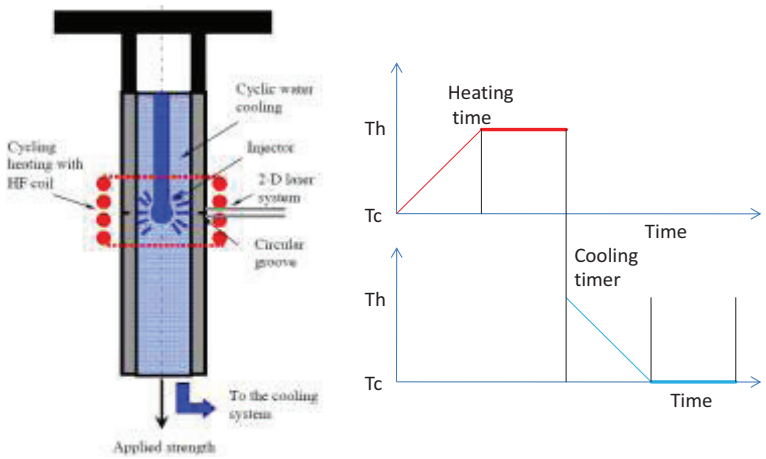

Figure 3. Principle schematic of the test device and thermal cycle.

Stress calculations (Fig. 4) clearly emphasize that a local heating is very well-adapted in the present case, since the external wall is mainly submitted to tensile stresses. In fact, such behavior results from component constraining effect: the part not heated leads to severe constraining conditions, and induces bending stresses. Calculations show that maximum stresses and constraining effect are obtained for a 30 mm length of local heating (15 mm for the half-specimen) as it is presented in Fig. 5.

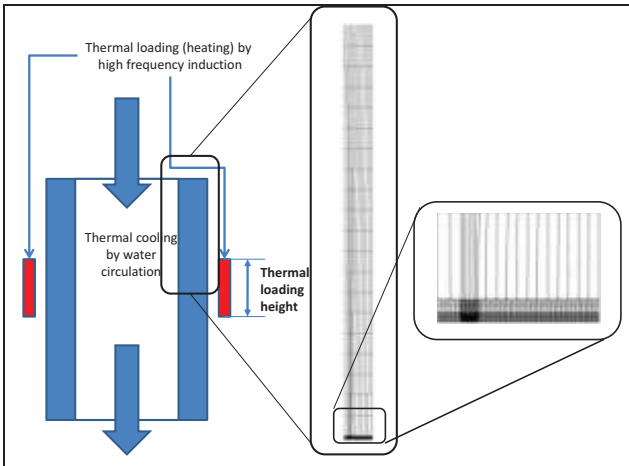

Figure 4. Axis-symmetrical finite element meshing of the pipe wall.

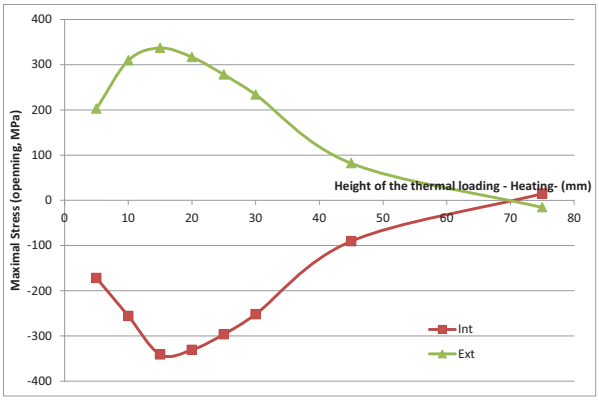

Figure 5. Evolution of the maximum axial stress as a function of the half-length of the heated zone.

Additional mechanical loading

A uniform tensile stress is applied to the specimen thanks to a 200 kN electro-mechanics tensile machine. The PROFATH device is integrated between its columns, below the actuator, as shown in Fig. 6.

Instrumentation and controls

Data acquisition and test control are provided by the joint use of a NI CompacDAQ device and CEA specific software written with LABVIEW.
Heating is devoted to a 6 kW high frequency generator controlled by software through the 4/20 mA input of the generator. The water and air injection valves are also software controlled.

Accurate thermal mapping as a function of time is obtained from 0.5 mm diameter K-thermocouple acquisitions. Thermocouples are placed at several depths (attached on outer wall, and 5 and 9 mm deep from outer wall), axial (7 values) and angular (0, 120, 240°) positions (Fig. 7 and 8).

Figure 6. General view of the PROFATH device.

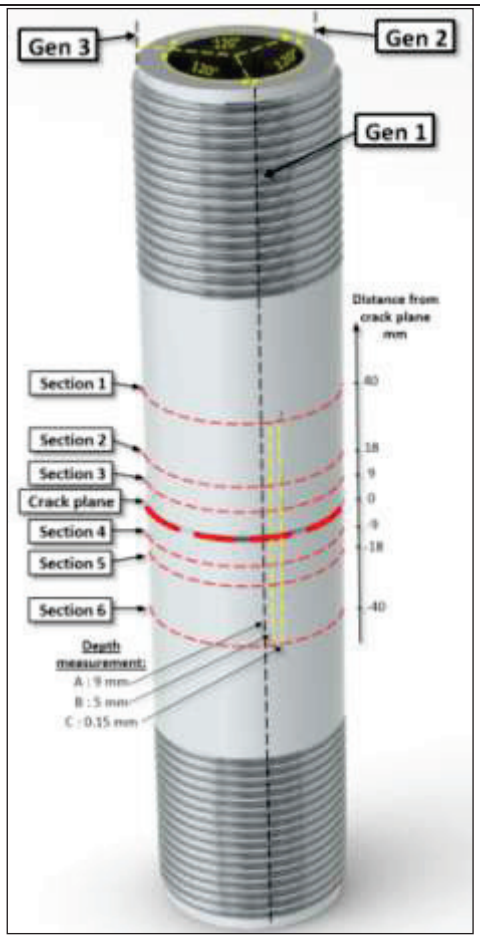

Figure 7. Location of the thermocouples.

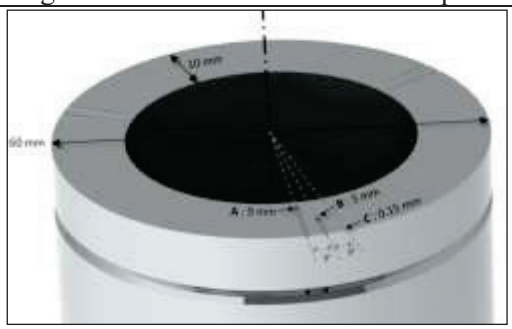

Figure 8. In-depth location of the thermocouples in section 3 (cut view).

Mechanical centering

Strain gauges are positioned at the lower part of the specimen to allow an initial optimal mechanical centering of the device (Fig. 9).

Crack length estimation

A compliance measurement is periodically done at three angular positions with an extensometer placed above the crack plane (Fig. 10), the specimen being slightly loaded with the electro-mechanics jack. Thanks to FE calculations, the equation linking compliance and crack length has been established.

Figure 9. Location of the strain gages for test n°2.

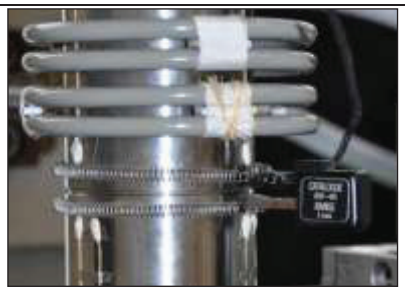

Figure 10. Crack length estimation by mechanical compliance with an INSTRON extensometer.

OPTIMISATION OF THE EXPERIMENTAL DEVICE

Cooling injectors

Many preliminary tests were performed with two types of water cooling injectors called "spherical injector" and "turning injector" and for different axial positions from the circular groove. Finally, chosen conditions are: a water flow rate of 12 l/min, a water coolant temperature of 17°C or less, a "spherical injector" placed at the circular groove plane. Such conditions give a cooling time of about 50 seconds.

Thermal map

The establishment of experimental thermal maps is required in order to qualify accurately the real thermal loads. A specific specimen instrumented with as many as 20 thermocouples is used. The thermocouples are placed at outer surface and at two depths within the wall thickness (respectively at 5 mm and 9 mm from the outer surface), and at three circumferential positions. Test specimens are instrumented with only 10 thermocouples, located at the outer surface and at 9 mm of this surface.
On the next two figures, the thermal loading is represented. Maximal temperature is effectively reached around the crack plane as illustrated in Fig. 11. Furthermore, the thermal loading remains truly axis-symmetrical during the entire test as shown in Fig. 12.

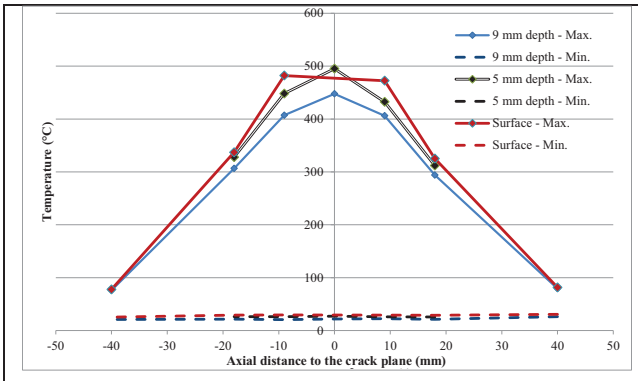

Figure 11. Axial evolution of the min/max temperature during a thermal cycle.

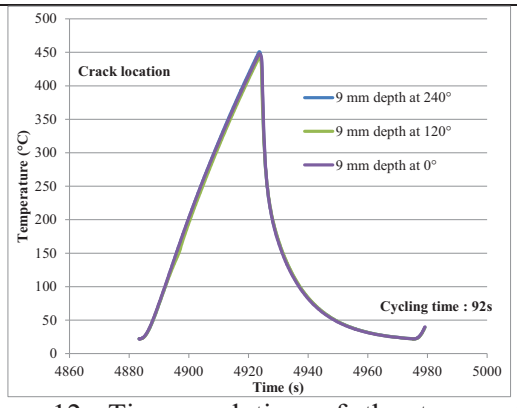

Figure 12. Time evolution of the temperature during a thermal cycle at different locations.

MAIN EXPERIMENTAL RESULTS

Four specimens have been tested. The first test was dedicated to develop and to validate the experimental protocol. This protocol has evolved through each test feedback and can finally be synthesized through the following steps:

- Instrumentation of the specimen (extra thermocouples, strain gauges…),
- Mechanical alignment of the specimen on the PROFATH device,
- Thermal cycling and static mechanical load,
- Mechanical compliance every 250/500 cycles to monitor the crack propagation: adjustment of test conditions for each step,
- Mechanical fatigue post cracking,
- Optical analysis of the fracture surface.

Table 1 presents the loading conditions used for the 3 first tests. An overview of the loading evolution and the final fracture surfaces is presented for tests 1 to 3 on Fig. 13. On the right left view, an enlargement of the fracture surface of the test 2 specimen is shown.

Table 1: Test loading conditions.

SPECIMEN Name	Precrak			Step 1			Step 2			Step 3		
	Length mm	Axial Load kN	Max T°C	Length mm	Axial Load kN	Max T°C	Length mm	Axial Load kN	Max T°C	Length mm	Axial Load kN	Max T°C
738A-B	1	200	500	1	150	450	2	100	450			
738C-B	1	190	450	1	190	400	2	150	400	2	100	400
738C-A	1	150	400	1	125	400	2	100	400	2	100	400

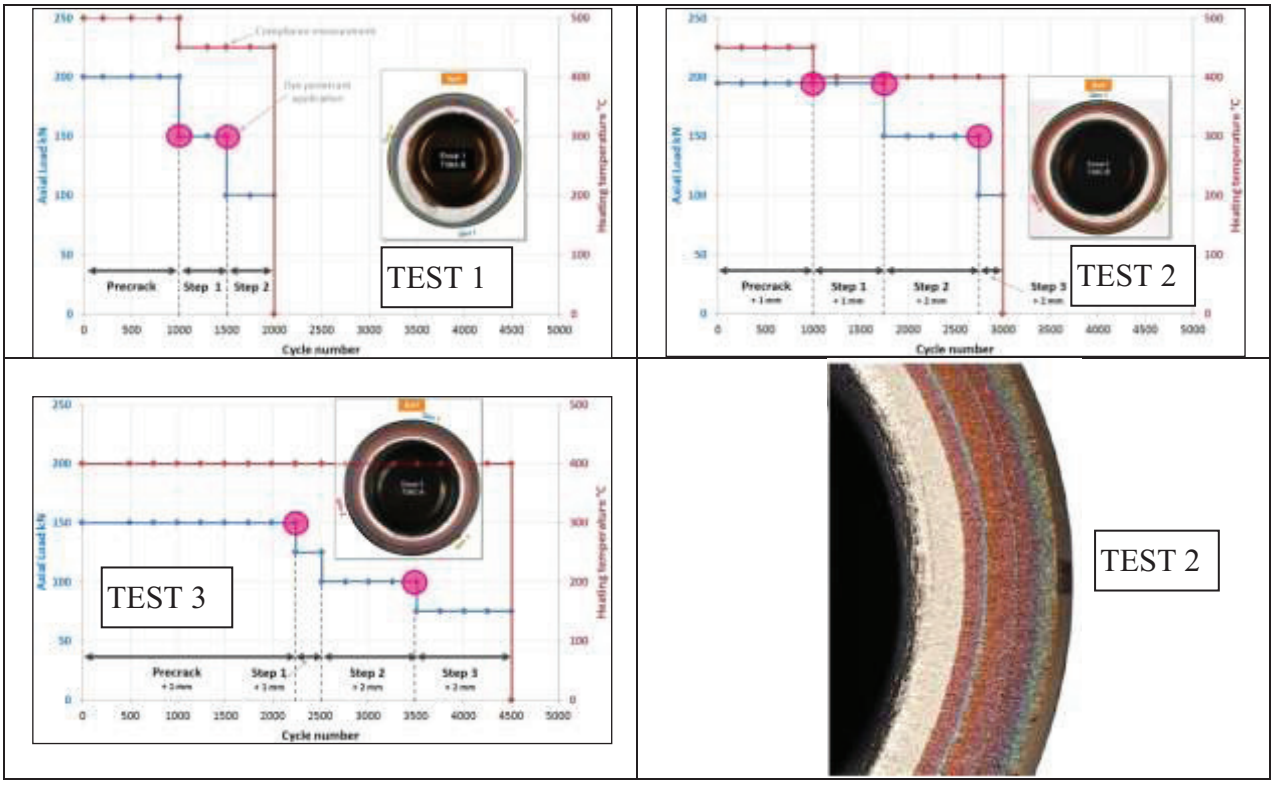

Figure 13. Overview of tests 1 to 3.

Post cracking is achieved by using a hydraulic device with a capacity of 500 kN. A cyclic displacement is imposed on the specimen with a ratio of 0.4. Application of dye penetrant product is performed for different intermediate steps during test (see Fig. 13). This one allows insuring optical measurements of the crack length after rupture. These post-mortem crack length values are in relative good agreement with estimates deduced from compliances.

TEST ANALYSIS

Due to the lack of space, the results of the crack growth rate tests under isothermal conditions at 20, 200 and 475°C will not be given here. There are presented in (Gourdin, 2015).

The thermo-mechanical calculations have been conducted using the CEA finite-element software Cast3M (Cast3M). Only a section of the PROFATH specimen has been modeled, since axis-symmetrical condition can be considered. 8-node quadratic elements are used. At the crack tip, a very refined mesh is used, since the element size is reduced to only 30 microns.

A first step deals with thermal calculations; the aim being to reproduce the experimental data obtained with thermocouples. Calculations are performed for the maximal temperatures of 400, 450 and 500°C chosen for the PROFATH program. The temperatures are measured with thermocouples placed at ± 9 mm axially from the crack plane. So, the maximal temperatures at the crack tip are systematically 30°C higher (Fig. 14); this difference is in good agreement with preliminary experimental measurements performed on the specific calibration specimen. Furthermore, an acceptable agreement can be observed between measurements and FE calculations at ± 9 mm (Fig. 15).

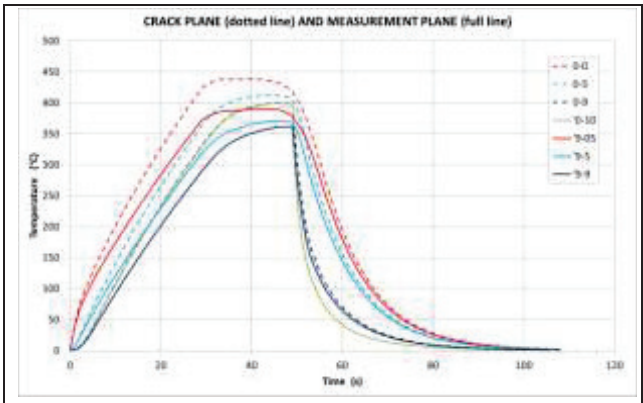

Figure 14. Calculated temperatures in the crack plane (dashed lines) and at ± 9 mm (solid lines), on the outer surface, 5 mm, and 9 mm depth.

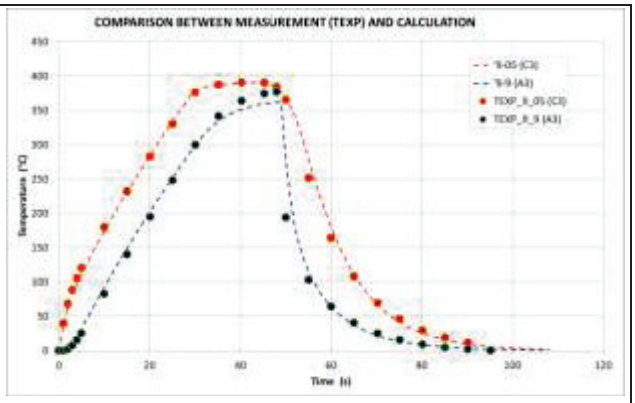

Figure 15. Comparison between estimated (dashed lines) and measured (dots) temperatures at ± 9 mm (axially) and at 9 mm depth.

In a second step, mechanical and fracture mechanics calculations are performed; crack lengths are based on compliance estimations. As generally done for analysis on components and proposed by the RSE-M approach, calculations have been made with an elastic behavior. Initial geometry is considered in the present calculations; such analysis will be probably revised in the future when a best knowledge of the diameter contraction will be available. Application of a Paris law requires both enough deep crack (referred as "mechanically long crack") and intermediate SIF values (≥15 MPa√m). In this frame, the analysis begins when a crack-growth of 1 mm is reached from the initial machined groove.

The stress intensity factor (SIF) is deduced from the energy release rate using the G-THETA procedure of Cast3M, considering a plane strain hypothesis. The maximum value of the SIF is reached when the

heating phase is ended; after, the SIF drops suddenly to a null value as soon as the water-injection starts; and it becomes equal to the mechanical component (K_{meca}) solely when the cycle is ended.

Fig. 16 compares the predicted number of cycles versus experimental ones at each compliance measurement for test 1 and test 2. Due to the non axis-symmetrical crack growth observed on test 1 specimen, the analysis has been conducted for three azimuths. This figure confirms that an elastic-plastic correction is required, since applying a simple elastic approach conducts to a large underestimation of the fatigue-life. Besides, it emphasizes a good agreement between experimental values and RSE-M predictions.

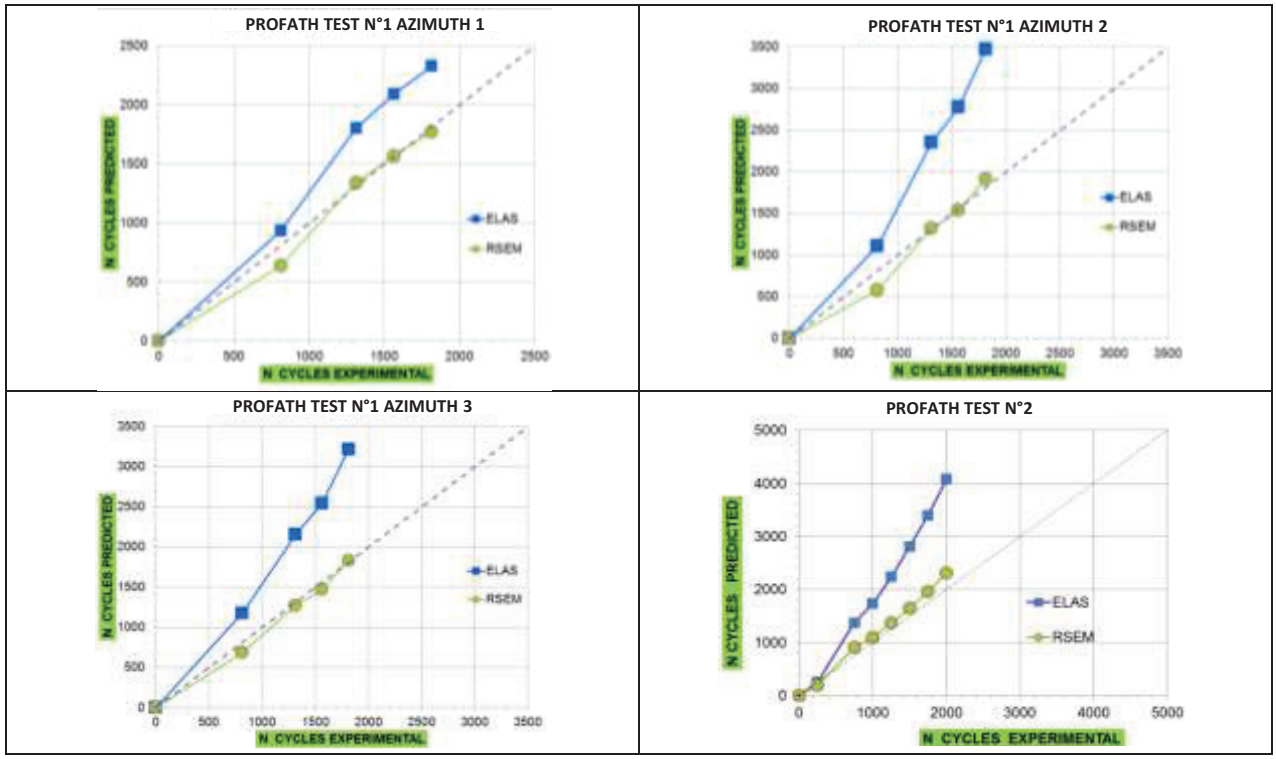

Figure 16. Predicted number of cycles versus experimental ones for tests n° 1 and n° 2.

A pure elastic fracture mechanics analysis conducts to large underestimates of the fatigue-life. Consequently, such a methodology is not acceptable for thermo-mechanical loading, when the plasticity at the crack-tip is not negligible, i.e. when $0.05\ (W\text{-}a) < r_{yA} \leq 0.085\ (W - a)$, where W-a is the un-cracked length, r_{yA} the cyclic plastic zone calculated using an Irwin's relation. The elastic-plastic correction proposed by the RSE-M Code conducts to accurate predictions.

CONCLUSION

In a first step, an isothermal fatigue crack growth test campaign was performed on CT-specimens with several loading conditions ($0.10 \leq R \leq 0.80$). This campaign shows that the application of a plastic correction (r_y and α coefficient) is not needed.

A new device called PROFATH was designed and built. Specimen is a thick-walled tube, and cyclic loads are applied: in a first part of the cycle, the external wall is heated by a high frequency induction coil, and in a second part of the cycle, heating is stopped and the internal wall is cooled by running water. Finite element calculations show that only a local axial portion of the tube must be submitted to cyclical thermal loads to guarantee an important structural effect. To be sure that only one crack will propagate, a sharp

circumferential groove is machined in the heated zone. A mechanical tensile loading may be also applied on the specimen with an electro-mechanical jack. Thermal mapping is deduced using a specific specimen instrumented with as many as 20 thermocouples, placed at the outer surface and within the wall thickness at two depth positions. Fatigue crack growth is measured by periodical compliance measurements and secured by injection of dye penetrant product at the end of each loading step.

After an experimental optimization phase, four tests have been performed on the PROFATH device. Some have already been assessed:

- The classical elastic estimation underestimates the crack propagation and is non-conservative,
- The RSE-M estimation provides an accurate crack propagation rate,
- Test n°4 (with a lower mechanical load) is achieved but not yet analyzed.

REFERENCES

AFNOR A 03-404 Standard (1991). "Pratique des essais de fissuration par fatigue," AFNOR

Ancelet, O., and al (2007). "Development of a test for the analysis of the harmfulness of a 3D thermal loading in tubes," *International Journal of Fatigue*, 29, pp. 549-564

ASTM E 647 (1995). "Standard Test Method for Measurement of Fatigue Crack Growth Rates," *American Society for Testing and Materials*

Bouin, P., Fissolo, A., Gourdin, C. (2010). "An experimental and numerical methodology to investigate on crack growth in a 304-L austenitic stainless steel pipe under thermal fatigue," *Proceedings of the ASME 2010 PVP Conference*, Bellevue, Washington, USA

Cast3M documentation. http://www-cast3m.cea.fr/

Cipière, M.F., Le Duff, J.A. (2001). "Thermal fatigue experience in French piping," *International Institute of Welding*, Document n°XIII-1981-01, Lubjana

Fissolo, A., Marini, B., Nais, G., Wident, P (1996). "Thermal fatigue behaviour for a 316 L type steel," *Journal of Nuclear Materials*, Vol. 233 – 237, pp. 156 – 161

Fissolo, A., Marini, B. (1998). "Multiple Cracking in Thermal Fatigue," *Proceedings 12th European Congress on Fracture*, p. 31, Sheffield, UK

Fissolo, A. (2001) "Fissuration en fatigue thermique des aciers inoxydables austénitiques", *CEA Report R-5982, Mémoire d'Habilitation à Diriger les Recherches*. Université des Sciences et Technologie de Lille.

Fissolo, A., Gourdin, C., Vincent, L. (2009). "Crack initiation under Thermal Fatigue: An Overview of CEA experience," *35th MPA Seminar*, 9 October 2009, Stuttgart (Germany)

Gourdin, C. et al (2015). "Investigations on crack propagation under cyclical isothermal and thermo-mechanical loadings for a type 304L stainless steel used for pressurized water reactors," *Proceedings of the ASME 2015 PVP Conference*, Boston, USA, paper PVP2015-45290

Nulife project (2008). "Pilot project on thermal fatigue – item 3", Document D(08) 25383, December 2008

RCC-MRx Code (2012). "Design and Construction Rules for Mechanical Components of High Temperature Nuclear Reactors and ITER Vacuum Vessel", 2012 Edition, AFCEN, Paris

RSE-M Code (2010). "Rules for In-service Inspection of Nuclear Power Plant Components", 2010 Edition and 2013 Addendum, AFCEN, Paris